International Geology Review

ISSN: (Print) (Online) Journal homepage: https://www.tandfonline.com/loi/tigr20

Post-volcanic activities in the Early Miocene Kırka-Phrigian caldera, western Anatolia – caldera basin filling and borate mineralization processes

Cahit Helvacı , Yeşim Yücel-Öztürk , Ioan Seghedi & Martin R. Palmer

To cite this article: Cahit Helvacı , Yeşim Yücel-Öztürk , Ioan Seghedi & Martin R. Palmer (2020): Post-volcanic activities in the Early Miocene Kırka-Phrigian caldera, western Anatolia – caldera basin filling and borate mineralization processes, International Geology Review, DOI: 10.1080/00206814.2020.1793422

To link to this article: https://doi.org/10.1080/00206814.2020.1793422

Published online: 23 Jul 2020.

INTERNATIONAL GEOLOGY REVIEW
https://doi.org/10.1080/00206814.2020.1793422

Taylor & Francis
Taylor & Francis Group

ARTICLE

Post-volcanic activities in the Early Miocene Kırka-Phrigian caldera, western Anatolia – caldera basin filling and borate mineralization processes

Cahit Helvacı[a], Yeşim Yücel-Öztürk[a], Ioan Seghedi[b] and Martin R. Palmer[c]

[a]Dokuz Eylül Üniversitesi, Mühendislik Fakültesi, Jeoloji Mühendisliği Bölümü, Tınaztepe Yerleşkesi, İzmir, Turkey; [b]Institute of Geodynamics, Romanian Academy, Bucharest, Romania; [c]School of Ocean and Earth Science, University of Southampton, National Oceanography Centre, European Way, Southampton, UK

ABSTRACT

The formation of large, economic borate deposits requires a boron-rich source, the means of transporting and concentrating the boron in a restricted environment, and mechanisms for the preservation of the deposit. There are several Miocene basins in western Turkey containing world-class borate reserves, with mineralization present as stratabound deposits in volcano-sedimentary successions. Although it is well-documented that the conditions required to form and preserve large borate deposits are most common in post-collisional tectonic settings (of which western Anatolia is a prime example), recent advances in the understanding of extensional tectonics and volcanism in this region, make it possible to gain fresh insights into their formation. Here, we suggest that formation of one of the largest borate deposits in the world was intimately related to the recently recognized Kırka-Phrigian caldera that lies in the northernmost part of the Miocene Eskişehir–Afyon volcanic field. Following caldera collapse, the basin filled with lacustrine sediments and volcaniclastic deposits with the boron mineralization concentrated in two main sub-basins: Sarıkaya and Göcenoluk. The close spatial and temporal relationship between borate deposition and the vast Early Miocene ignimbrite deposits that surround the caldera (and contain high levels of elements associated with mineralization) strongly suggest that the ignimbrites were the major source of boron. The boron was transported by geothermal fluids and post-volcanic gases that vented into warm water at the base of the caldera-paleolake system and was then concentrated during cycles of sedimentation and evaporation, with most of the mineralization concentrated along a N-S striking fault system.

ARTICLE HISTORY
Received 17 February 2020
Accepted 4 July 2020

KEYWORDS
Extensional tectonics; borate mineralization; early Miocene; Kırka-Phrigian caldera; western Anatolia

1. Introduction

Extension, crustal thinning and alkaline – calc-alkaline volcanism occurred throughout western Turkey during the Miocene (~20 – 10 Ma). Extension resulted in a series of N- to NE-trending, fault-bounded basins that formed on the northern part of the Menderes Massif and the adjacent İzmir-Ankara zone. Plutonic and volcanic rocks in western Anatolia were largely emplaced along NNE-SSW trending structures (Figure 1) (Yılmaz *et al*. 2000; Purvis and Robertson 2005; Karacık *et al*. 2007; Ersoy *et al*. 2010; Erkül and Erkül 2010; Karaoğlu *et al*. 2010). Continental sediments and the products of calc-alkaline volcanism filled these basins between 21 and 14 Ma (e.g., Yalçın 1988; Savaşçın and Oyman 1998; Dilek and Altunkaynak 2009, 2010; Seghedi *et al*. 2013). The lower Miocene terrestrial sediments, which are present within all the borate basins, were also deposited directly on high-grade metamorphic rocks that form the entire northern part of the Menderes Massif, as well as across contacts between the Menderes Massif and the surrounding tectonic units (e.g. the ophiolitic rocks of the İzmir-Ankara suture zone, Figure 2).

Borate deposits occur worldwide, but by far the most important, from a commercial standpoint are the Neogene to Holocene continental deposits of North America, the central Andes of South America and western Anatolia. These borate deposits all formed as evaporites or chemical precipitates in closed continental basins under arid to semi-arid conditions. The major deposits are all associated with volcanic rocks and thermal springs, which are the assumed sources and transport vectors of the boron (Kistler and Helvacı 1994; Smith and Medrano 1996; Garrett 1998; Helvacı and Alonso 2000; Helvacı and Palmer 2017). Three major geochemical groups of Tertiary borate deposits have been differentiated: (1) Ca- and Na-Ca-borate formations, characterized by colemanite and ulexite facies; (2) Na-borate formations, characterized by borax (and kernite) facies, and (3) Mg-bearing borate formations (Kistler and

CONTACT Yeşim Yücel-Öztürk yesim.yucel@deu.edu.tr Dokuz Eylül Üniversitesi, Mühendislik Fakültesi, Jeoloji Mühendisliği Bölümü, Tınaztepe Yerleşkesi, TR-35160 Buca, İzmir, TURKEY.

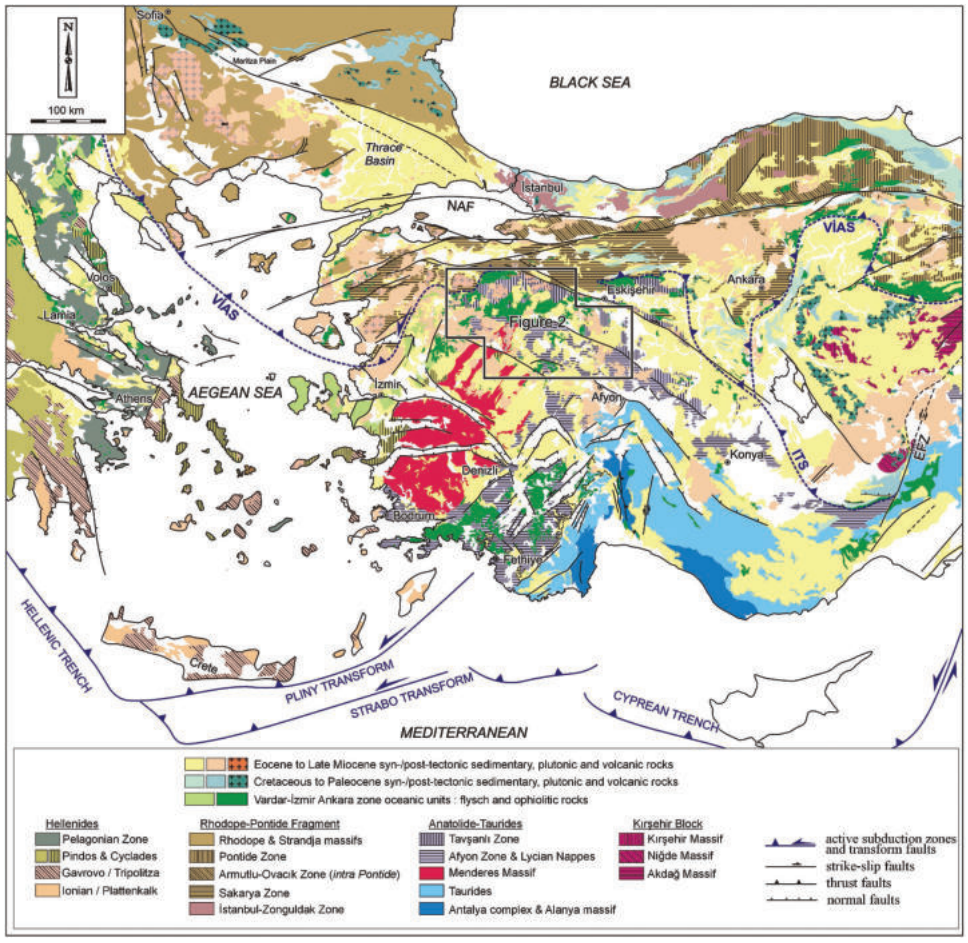

Figure 1. Simplified geologic map of western and central Anatolia, Turkey and the Aegean region showing major tectonic features and rock units. Abbreviations: EFZ: Ecemiş Fault Zone; NAF: north Anatolian Fault Zone; VIAS: Vardar–İzmir–Ankara Suture Zone. Modified from 1/500.000 scaled geological map of Turkey (MTA, 2002), and.Çemen *et al*. (2014)

Helvacı 1994; Smith and Medrano 1996; Helvacı and Palmer 2017; Helvacı *et al*. 2017).

The geometry, stratigraphy, tectonics and volcanic components of the borate bearing Neogene basins in western Anatolia offer important insights into the relationship between basin evolution, borate mineralization and mode of extension in western Anatolia (Figure 2). Most of the borate deposits developed in NE-SW trending basins developed along the İzmir-Balıkesir Transfer Zone (İBTZ) (e.g. Bigadiç, Sultançayır and Kestelek basins), or on the northern side of the Menderes Core Complex (MCC) (e.g. Selendi and Emet basins). In contrast, the Kırka borate deposit (that lies further to the east) is located inside a caldera (e.g., Seghedi and Helvacı 2016) (Figure 2). Petrographic features, composition and replacement relationships of the borate minerals (principally borax, with lesser amounts of colemanite and ulexite) and associated authigenic minerals have been described in the Kırka Sarıkaya deposit by İnan *et al*. (1973), Sunder (1980), Yalçın and Baysal (1991), Helvacı and Alonso (2000) and Helvacı and Orti (2004).

Here, we review the eruptive history of this caldera, the largest in the Eskişehir–Afyon area, and its relationship with the world-class borate formation within the collapse area which is named for the main city inside the edifice and its numerous historical artefacts belonging to Phrigian culture (Seghedi and Helvacı 2016). The main purpose of this study is to examine the relationship between the evolution of the caldera and the formation of the associated borate deposit.

2. Geological setting

Western Anatolia contains several continental blocks that were originally separated by the northern branch of the Neo-Tethyan ocean and is marked today by the Vardar-İzmir-Ankara Suture Zone (Figure 1). This suture zone separates the Sakarya continent to the north and the Anatolide–Tauride block to the south and was formed by late Mesozoic northward subduction and accretion (Şengör and Yılmaz 1981). The main continental blocks are the Sakarya zone of the Rhodope-Pontide

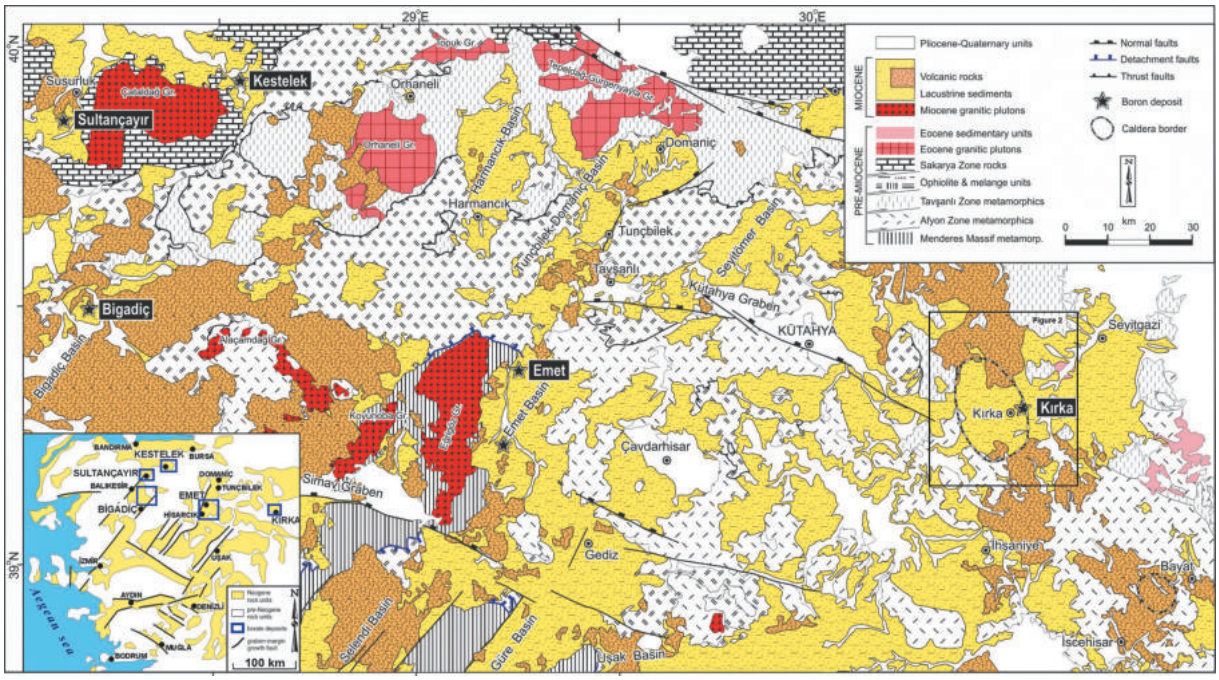

Figure 2. Simplified geological map of the Neogene basins and borate deposits located NE of the Menderes Massif in western Anatolia. The approximate location of the Kırka-Phrigian caldera is outlined.

Fragment (north) and the Menderes Massif of the Anatolides (south). The region has experienced continued tectonic evolution through subduction, obduction, continental collision and subsequent crustal thickening, followed by extension and crustal thinning between the continental blocks and suture zones (Şengör and Yılmaz 1981).

2.1. Pre-caldera basement rocks

The basement units of western Anatolia comprise: (1) the Menderes and Cycladic massifs, (2) the İzmir-Ankara Zone (comprising; (a) the Bornova flysch zone, (b) the Afyon zone, and (c) the Tavşanlı zone), (3) the rocks of the Sakarya Continent to the north, and (4) the Lycian Nappes to the south (Şengör and Yılmaz 1981). The Afyon zone comprises of a Devonian to Palaeocene clastic and carbonate shelf sequence metamorphosed to greenschist facies. The Tavşanlı Zone is represented by Palaeozoic metamorphic rocks, a Mesozoic ophiolite complex and Eocene fossiliferous limestone (Figure 1; Okay and Satır 2006; Okay 2011). In the Kırka area, these units are unconformably overlain by unmetamorphosed Lower Eocene shallow water marine sediments consisting of siltstones, marly limestones and limestones (Özcan *et al*. 1988). The Kırka-Phrigian caldera is situated over the basement between the Tavşanlı and Afyon Zones, and is surrounded by Palaeozoic metamorphics, a Mesozoic ophiolite complex and Eocene marine fossiliferous limestone (Floyd *et al*. 1998; Seghedi and Helvacı 2016) (Figure 3).

2.2. Caldera Formation and Caldera related volcanic rocks

Ignimbrites are the most voluminous volcanic deposits related to caldera formation (Figure 3; Floyd *et al*. 1998; Seghedi and Helvacı 2016). Although these are distributed all around the caldera, the best preserved and most abundant outflow ignimbrites are mostly on the south side (e.g. Keller and Villari 1972; Floyd *et al*. 1998; Seghedi and Helvacı 2016). The ignimbrites have been dated at ~18.6 Ma from a sample taken ~20 km south of the caldera margin where ignimbrites lie directly on pre-tertiary basement rocks (Anderson 1997). The caldera is roughly oval (24 km x 15 km) in shape and is thought to have formed during collapse events, at the time of initial ignimbrite eruption (Figure 3; Floyd *et al*. 1998; Seghedi and Helvacı 2016). The initial eruption formed the Rhyolite-1 ignimbrites, which show features of rapid agglutination, welding, and rheomorphism, consistent with a high discharge rate and a short period of emplacement (e.g., Lavallée *et al*. 2015).

The base of the volcanic sequence forms a 160–200 m thick exposure (including the caldera-forming ignimbrites) at the structural margin of the caldera and is generally made up of ignimbrites and lag breccias (Figure 4(a,b); (Floyd *et al*. 1998; Seghedi and Helvacı

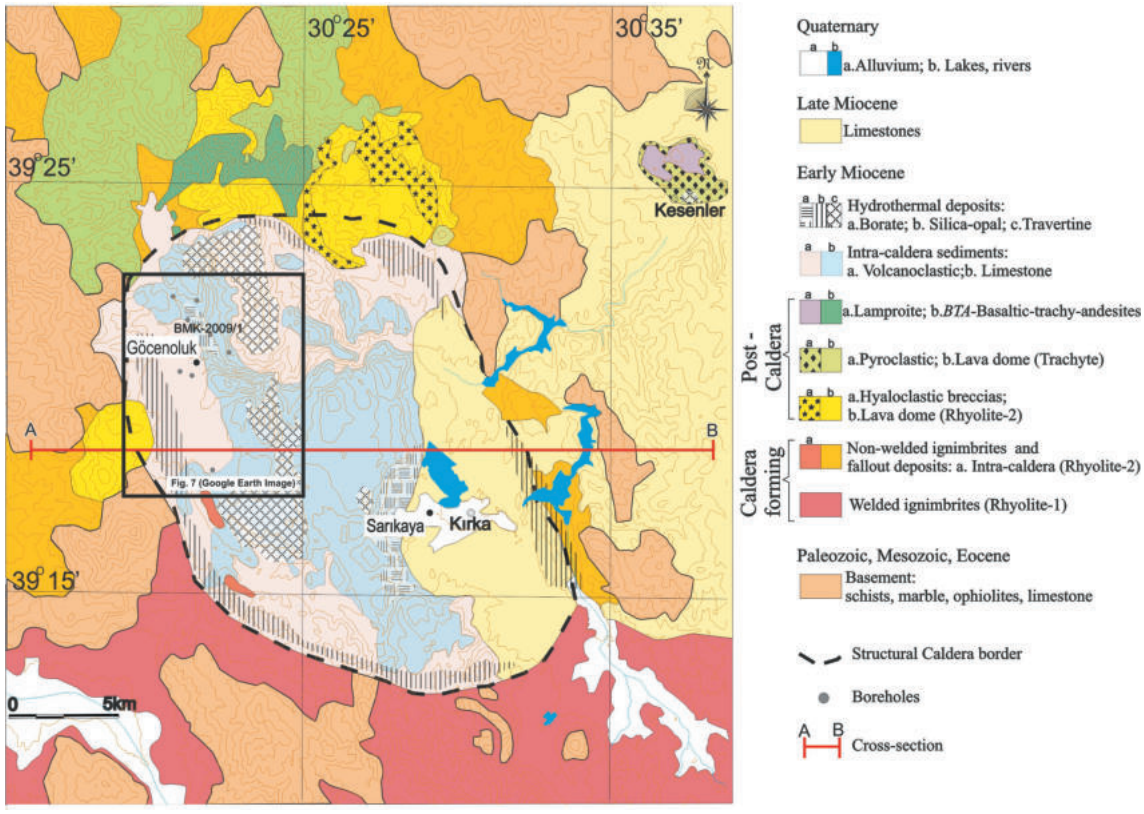

Figure 3. Geological map of the Kırka-Phrigian caldera with 50 m contours (after.Seghedi and Helvacı 2016). The inset shows the study area at the northern edge of the Isparta angle in the context of a simplified tectonic map of the eastern Mediterranean. Drilling locations on the map are marked as grey dots. The individual boreholes are labelled in the right-hand panel of Figure 8

2016). The slightly to moderately welded ignimbrite facies (Figure 4(c)) is well-represented outside the east, north and west sides of the caldera and is always associated with thick fall-out deposits (Figure 4(e,f)). The second major collapse event resulted from a series of Plinian eruptions which formed pyroclastic rocks and thick fall-out deposits located to the north of the caldera. These flows (Rhyolite-2) generated both intra-and extra-caldera ignimbrites, and contain welded and non-welded facies (Figure 3) (Seghedi and Helvacı 2016).

The intra-caldera ignimbrite occurs as smaller outcrops towards the southwestern part of the caldera (Figure 3). They are weakly welded and are similar to the ignimbrites distributed outside the caldera walls to the east, west and north (Figure 4(a,b)). The last stage of rhyolitic volcanism generated a thick deposit of fall-out tuffs with accretionary lapilli (Figure 4(d)), suggesting that this late eruption was triggered by magma-water interaction. The water likely accumulated in the collapse basin of the Kırka-Phrigian caldera.

K-Ar dating on biotite from the Rhyolite-1 ignimbrite yields ages ranging from 18.5 ± 0.2 to 19.0 ± 0.2 Ma (Helvacı and Alonso 2000). More recent $^{40}Ar/^{39}Ar$ dates from the Rhyolite-2 ignimbrite, from the bottom of the caldera (sample no. K-6, from Seghedi and Helvacı 2016), the eastern side (K50B) and a ring fracture dome situated in the north (sample no. KG-91, from Seghedi and Helvacı 2016) yield age of 18.72 ± 0.04 Ma, and suggest closely spaced (<0.2 Ma) eruption events (Seghedi and Helvacı 2016) (Table 1). Lack of erosional features also implies that the ignimbrites of Rhyolite-2 closely followed the Rhyolite-1 ignimbrites and are indicative of a short period for caldera collapse generation.

2.3. *Post-caldera (post-collapse) volcanic rocks*

Post-collapse volcanism was initially dominated by emplacement of rhyolitic domes and was followed by trachytic domes that partially overlie the rhyolitic domes (Figure 3). The rhyolite domes that formed at the northern rim of the caldera are surrounded by a hyaloclastite breccia envelope that suggests a subaqueous environment during dome emplacement (more detail explanation given in Seghedi and Helvacı 2016).

Post-caldera effusive basaltic-trachy-andesites (BTA) and the Kesenler lamproite volcano (situated 8 km NE from the caldera border) yield $^{40}Ar/^{39}Ar$ ages of 16.92

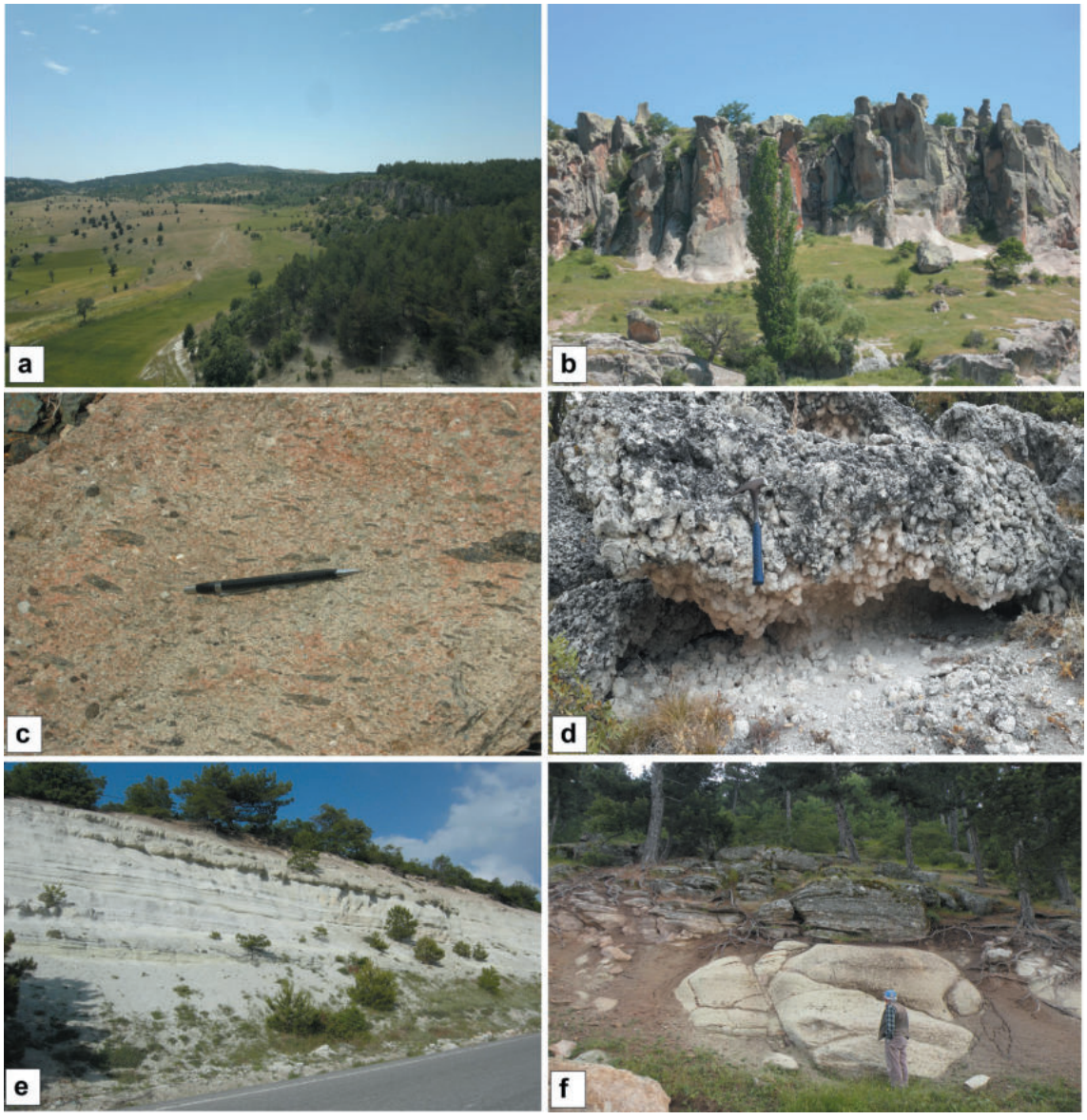

Figure 4. Volcanology field photographs: (a) Caldera wall in the west of the Kırka – Phrigian caldera; (b) thick basal sequence of welded ignimbrites seen from the south, showing vertical columnar jointing; (c) a detail of a rheomorphic flow deposit with dark glassy fiamme; (d) thick accretionary lappili deposit at the south-eastern margin of the caldera; individual rounded lapilli may reach 6 cm in diameter. (e) thick succession of fall-out deposits outside the caldera in the north-western part; (f) layered pyroclastic fall and surge deposits at the top of a thick pyroclastic flow deposit outside caldera in its southern part.

Table 1. K/Ar and $^{40}Ar/^{39}Ar$ age datings in the Kırka-Phrigian caldera.

Events	Ages	References
Rhyolite-1	18.5 ± 0.2-biotite (K/Ar)	Helvacı and Alonso (2000)
	19.0 ± 0.2 Ma-biotite (K/Ar)	Helvacı (1995)
Rhyolite-2	18.59 ± 0.05 Ma; 18.83 ± 0.07 Ma (KG-50b, average)	Seghedi and Helvacı (2016)
	18.69 ± 0.04 Ma ($^{40}Ar/^{39}Ar$) (K-6)	
	18.72 ± 0.04 ($^{40}Ar/^{39}Ar$) (KG-91, average)	
Basalt	18.63 ± 0.04 ($^{40}Ar/^{39}Ar$)	Seghedi and Helvacı (2016)
Basaltic-trachy-andesite	– – – – – – – – – – **end of collapse events**	
	16.92 ± 0.05 Ma ($^{40}Ar/^{39}Ar$)	
Lamproite	16.21 ± 0.02 Ma ($^{40}Ar/^{39}Ar$)	Seghedi and Helvacı (2016)

and 16.21 Ma, respectively (Table 1; Seghedi and Helvacı 2016). This suggests that these primitive volcanic products are the youngest dated units and that they were generated ~1 Myr after the rhyolites. This evolution

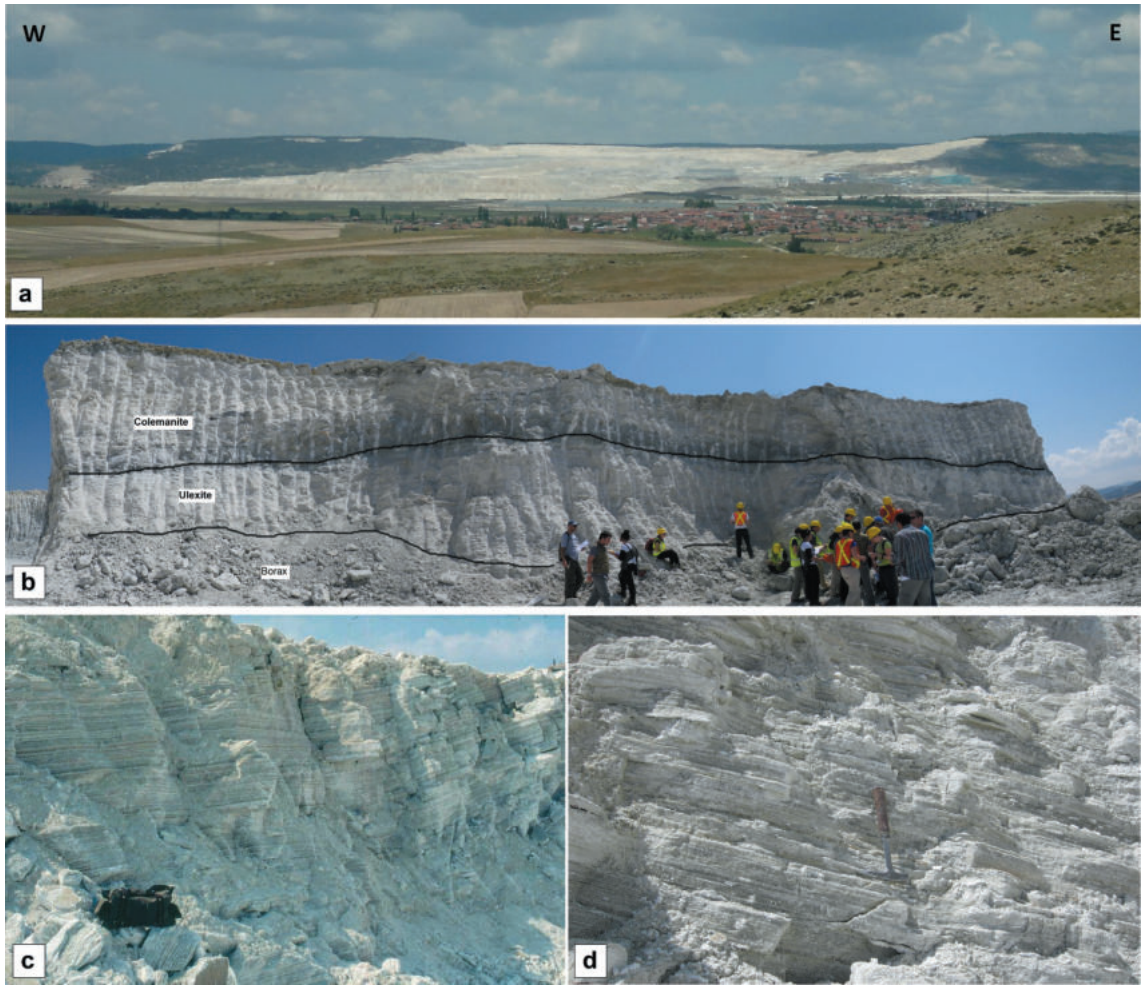

Figure 5. (a) Kırka Sarıkaya opencast borax mine, Eskişehir county; (b) View of Sarıkaya quarry with ulexite layers alternating with nodular and massive lithofacies of colemanite. Crystalline masses, vugs, geodes, and veins can be observed, in the upper section of the Sarıkaya opencast deposit; (c) Alternating borax layers and dolomitic clays; (d) Laminated lithofacies of borax (brown material) alternating with dolomitic, marly laminae (white laminae). Laminated borax lithofacies with palisade fabric in borax laminae. Clear material corresponds to lutitic matrix and laminae (dolomitic claystone). Dark material corresponds to fresh, crystalline borax.

from calc-alkaline rhyolites and associated products to transitional high-Mg basaltic, trachytic and lamproitic compositions has also been documented in the Eskişehir–Afyon volcanic field (north Anatolia) and the Miocene volcanics associated with the Menderes Massif core complex extension (Akal *et al*. 2013; Aydar *et al*. 1998; Prelević *et al*. 2012; Ersoy and Palmer 2013; Seghedi *et al*. 2013).

2.4. Post-caldera basin-filling deposits

Caldera formation was followed by reworking of the volcaniclastic deposits, emplacement of occasional interbedded lavas or sills, and late-stage hydrothermal activity that produced silica and borate mineralization and crosscutting travertine deposits (Figures 5 and 6). Secondary silica deposition and sub-vertical opaline silica veins also occur along caldera walls.

Caldera fill deposits consist of claystones, mudstones, sandstones and dolomitic limestones are intercalated with volcaniclastic and borate deposits (Figure 7; detailed explanation given in Seghedi and Helvacı 2016). Drilling in the Gocenoluk area intersected a thick succession of dolostones, tuffs and three separate borate-bearing units (Lower, Intermediate and Upper Borate Units, Figure 8) (García-Veigas and Helvacı 2013; Seghedi and Helvacı 2016). Outcrops and boreholes of the top of caldera basinal deposits display a variety of erosional contacts.

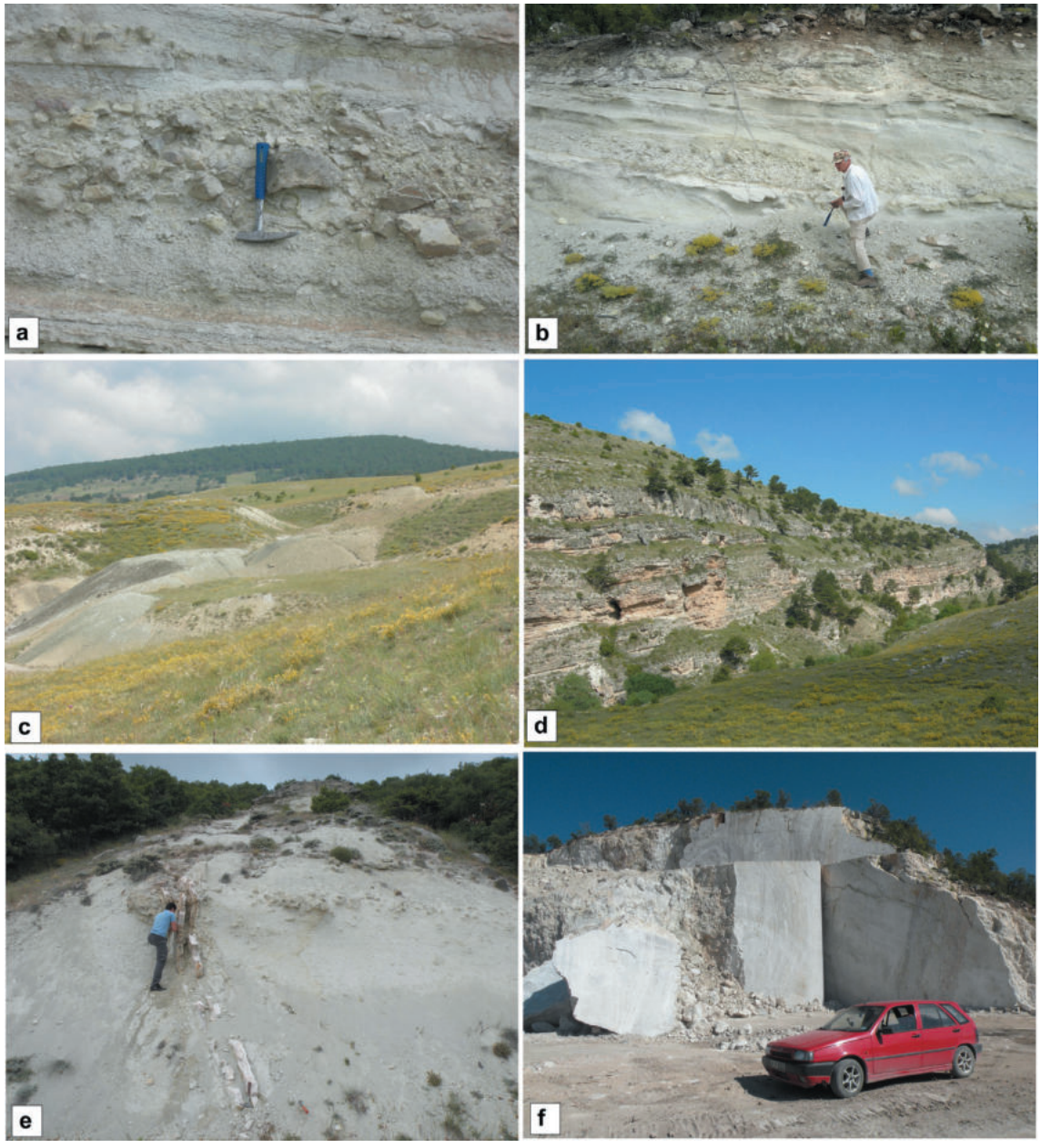

Figure 6. Intra-caldera sedimentary deposits: (a) massive poorly sorted sandstone and conglomerate succession close to the north-western side of the caldera; (b) low-angle trough or scour-fill cross-bedded breccias in the north-western side of the caldera interior; (c) Old mine side of the Göcenoluk deposit; (d) Thick capping limestone between the Göcenoluk and Sarıkaya borate areas. See also Figures 2 and 3. Intra-caldera hydrothermal deposits (e) N-S oriented vertical travertine vein cutting epiclastic deposits in the northwestern part of the caldera interior; (f) Thick N-S oriented vertical travertine vein cutting upper limestone deposits in the south eastern part of the caldera interior (photo from Seghedi and Helvacı 2016).

2.5. Hydrothermal deposits: boron mineralization and silica and travertine formation

The borate deposits are located in the interior of the caldera, following a ~ N-S trending fault system likely formed during post-caldera tectonic reactivation probably caused by magma resurgence or regional tectonism. The maximum age of the borate mineralization is constrained by the basal Rhyolite-2 ignimbrite (18.59 ± 0.05 Ma; 18.83 ± 0.07 Ma) and the minimum age is constrained by the post-caldera effusive basaltic trachyandesites (16.92 ± 0.05 Ma) (Table 1; Seghedi and Helvacı 2016). The initial boron enrichment likely derived from leaching of the volcanic rocks in the caldera by hot meteoric waters and post-caldera hydrothermal degassing to produce solutions that were also variably enriched in Li, S, Sr and As (e.g. İnan *et al*. 1973; Yalçın and Baysal 1991; Helvacı and Orti 2004; Özkul 2008;

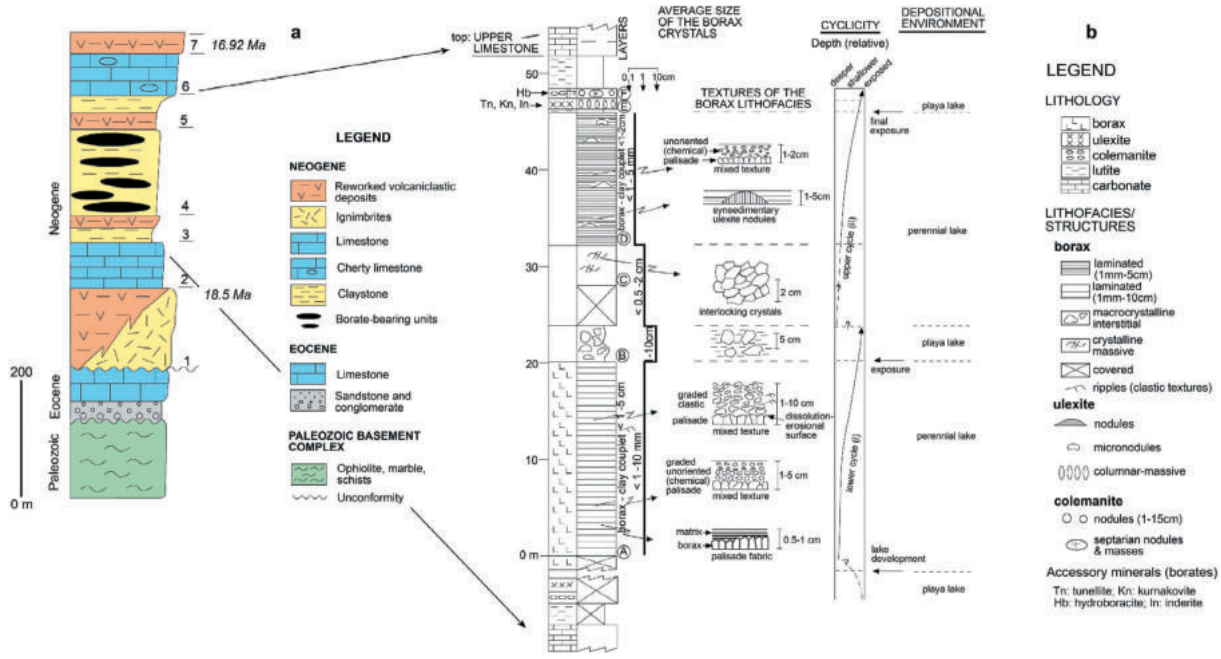

Figure 7. (a) Simplified stratigraphic column of the Kırka borate deposit. Neogene rock units: 1: Tuffs, 2: Lower limestone, 3: Lower clay, marl and tuff, 4: Borate unit, 5: Upper clay, tuff, marl and coal bands, 6: Upper cherty limestone, 7: Basaltic trachyandesite (Seghedi and Helvacı 2016). (b) Lithological log of Section 2, in the central part of the Kırka borate unit (modified from Helvacı and Ortí 2004).

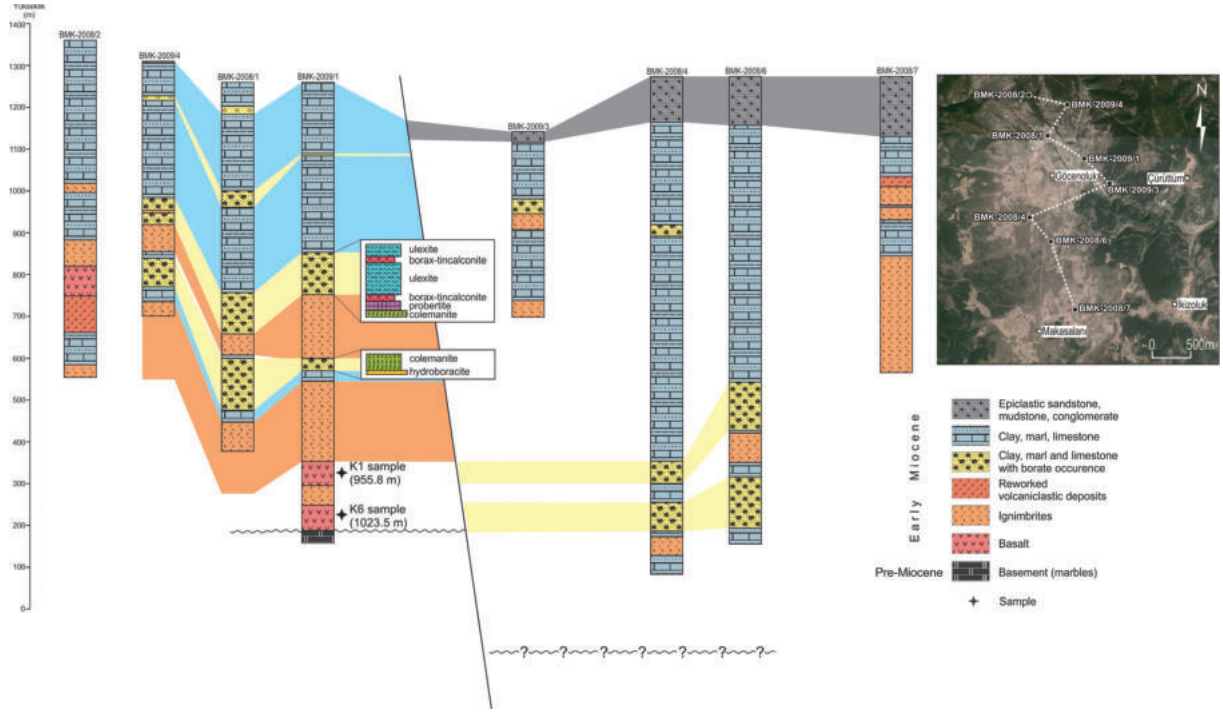

Figure 8. Lithology of the drill cores obtained by Eti Mine Company for borate deposits in the Göcenoluk area. The location of the drill cores is shown in a Google map in the top right-hand panel and also marked on.Figure 3

Koçak and Koç 2012, 2016, 2018; García-Veigas and Helvacı 2013; Seghedi and Helvacı 2016; Koc *et al*. 2017; Özkul et al. 2017).

Travertine precipitation from hot springs forms N-S oriented vertical or subvertical veins that range in size from several cm up to 10 m wide, and cut the epiclastic and limestone deposits in the northwest part of the caldera interior. This area also contains the Kırka Sarıkaya borate deposit, where there is a quarry that mines several travertine veins cross-cutting the borate unit and the overlying limestone (Figure 6(f)). There are also several travertine veins in the southeast part of the Kırka town and in the northwest of the Göcenoluk area (Figure 6(e)). The Kırka borate area consists of two main outcropping areas near the villages of Sarıkaya and Göcenoluk (Figure 7).

2.6. Kırka Sarıkaya borate deposit

Kırka Sarıkaya is the largest borax ore body in Turkey and has a B_2O_3 content of 20–25 wt.%. The deposit is hosted by sedimentary rocks that were deposited in the Kırka Phrigian caldera and form a succession >400 m thick. The succession is composed of the following units from base to top: volcanic rocks and tuffs (80 m), lower limestone (80 m), lower clay horizon with interbedded marls and tuffs (40 m), borate unit (70–145 m), upper claystones with tuff, marl and thin coal bands (60 m), and an upper limestone (>50 m) (Figure 7, İnan 1972; Sunder 1980; Helvacı and Alonso 2000; Helvacı and Ortí 2004). The borate succession lies in the central part of the Sarıkaya basin where it forms a unit up to 145 m thick, where it is exposed in the opencast mine (Figure 7). Overburden ranges from 5 to 130 m thick and consists principally of claystones and limestones. The deposit contains a borax body (>50 m thick) that is enveloped by a thin ulexite-dominant facies and a more distal colemanite-dominant facies and dolomitic claystone, with other Ca-, Na-, Mg- and Sr-borates present in subordinated amounts (Table 2; İnan *et al*. 1973; Sunder 1980; Helvacı and Ortí 2004). Dolomite is the main carbonate, with minor amounts of magnesite and calcite, and rare strontianite.

The borate unit consists of the following layers or intervals, in ascending order (Helvacı and Ortí 2004): colemanite; ulexite; laminated borax; interstitial macrocrystalline borax; massive crystalline borax; laminated borax, with lenticular nodules of ulexite; fibrous, columnar ulexite, with Mg-bearing borates (inderite, kurnakovite); nodular to massive colemanite. In addition, hydrochloroborite, brianroulstonite, hilgardite-4 M and searlesite were reported by Kocak and Koç (2016). This vertical succession is almost symmetrically zoned as colemanite – ulexite – borax – ulexite – colemanite (Figure 7), with claystones and tuffs interbedded between the borate layers. Overall, the marl/clay horizon containing the borate ore body strikes NNE and dips about 18–20° to the WNW , limited by the caldera border (Figure 3).

Borax is the dominant primary borate mineral and was originally deposited as thin crystal beds, as indicated by sedimentary structures and crystal habits in the Na-borate facies in the deposit. These features indicate that most of the borax precipitated directly from the caldera lake brine in beds 3–100 mm thick within thin-bedded

Table 2. Borate minerals, formulas and chemical composition occurring in the Kırka borate basin.

	Structural formula	Empirical formula	Oxid like formula
CA-BORATES			
PRICEITE (PANDERMITE)	$Ca_2(B_5O_7(OH)_5).H_2O$	$Ca_4B_{10}O_{19}.7H_2O$	4CaO 5B2O3 7H2O
COLEMANITE	$Ca(B_3O_4(OH)_3).H_2O$	$Ca_2B_6O_{11}.5H_2O$	2CaO 3B2O3 5H2O
MEYERHOFFERITE	$Ca(B_3O_3(OH)_5).H_2O$	$Ca_2B_6O_{11}.7H2O$	2CaO $3B_2O_3$ $7H_2O$
INYOITE	$Ca(B_3O_3(OH)_5).4H_20$	$Ca_2B_6O_{11}.13H2O$	2CaO $3B_2O_3$ $13H_2O$
CA-NA-BORATES			
PROBERTITE	$NaCa(B_5O_7(OH)_4).3H_2O$	$NaCaB_5O_9.5H_2O$	Na_2O 2CaO $5B_2O_3$ $10H_2O$
ULEXITE	$NaCa(B_5O_6(OH)_6).5H_2O$	$NaCaB_5O_9.8H_2O$	Na_2O 2CaO $5B_2O_3$ $16H_2O$
NA-BORATES			
KERNITE	$Na_2(B_4O_6(OH)_2).3H_2O$	$Na_2B_4O_7.4H_2O$	Na_2O $2B_2O_3$ $4H_2O$
TINCALCONITE	$Na_2(B_4O_5(OH)_4).3H_20$	$Na_2B_4O_7.5H_2O$	Na_2O $2B_2O_3$ $5H_2O$
BORAX	$Na_2(B_4O_5(OH)_4).8H_20$	$Na_2B_4O_7.10H_2O$	Na_2O $2B_2O_3$ $10H_2O$
MG-BORATES			
KURNAKOVITE	$Mg(B_3O_3(OH)_5).5H_2O$	$Mg_2B_6O_{11}.15H_2O$	2MgO $3B_2O_3$ $15H_2O$
INDERITE	$Mg(B_3O_3(OH)_5).5H_2O$	$Mg_2B_6O_{11}.15H_2O$	2MgO $3B_2O_3$ $15H_2O$
MG-CA-BORATES			
HYDROBORACITE	$CaMg(B_6O_8(OH)_6).3H_2O$	$CaMgB_6O_{11}.6H_2O$	CaO MgO $3B_2O_3$ $3H_2O$
INDERBORITE	$CaMg(B_3O_3(OH)_5)_2.6H_2O$	$CaMgB_6O_{11}.11H_2O$	CaO MgO $3B_2O_3$ $11H_2O$
SR-BORATES			
VEATCHITE-A	$Sr_2(B_{11}O_{16}(OH)_5).H_2O$	$Sr_4B_{22}O_{37}.7H_2O$	4SrO $11B_2O_3$ $7H_2O$
TUNELLITE	$Sr(B_6O_9(OH)_2).3H2O$	$SrB_6O_{10}.4.H_2O$	SrO $3B_2O_3$ $4H_2O$
BOROSILICATES			
SEARLESITE	$NaBSi_2O_5(OH)_2$	$NaBSi_2O_6.H_2O$	Na_2O B_2O_3 $4SiO_2$ $2H_2O$

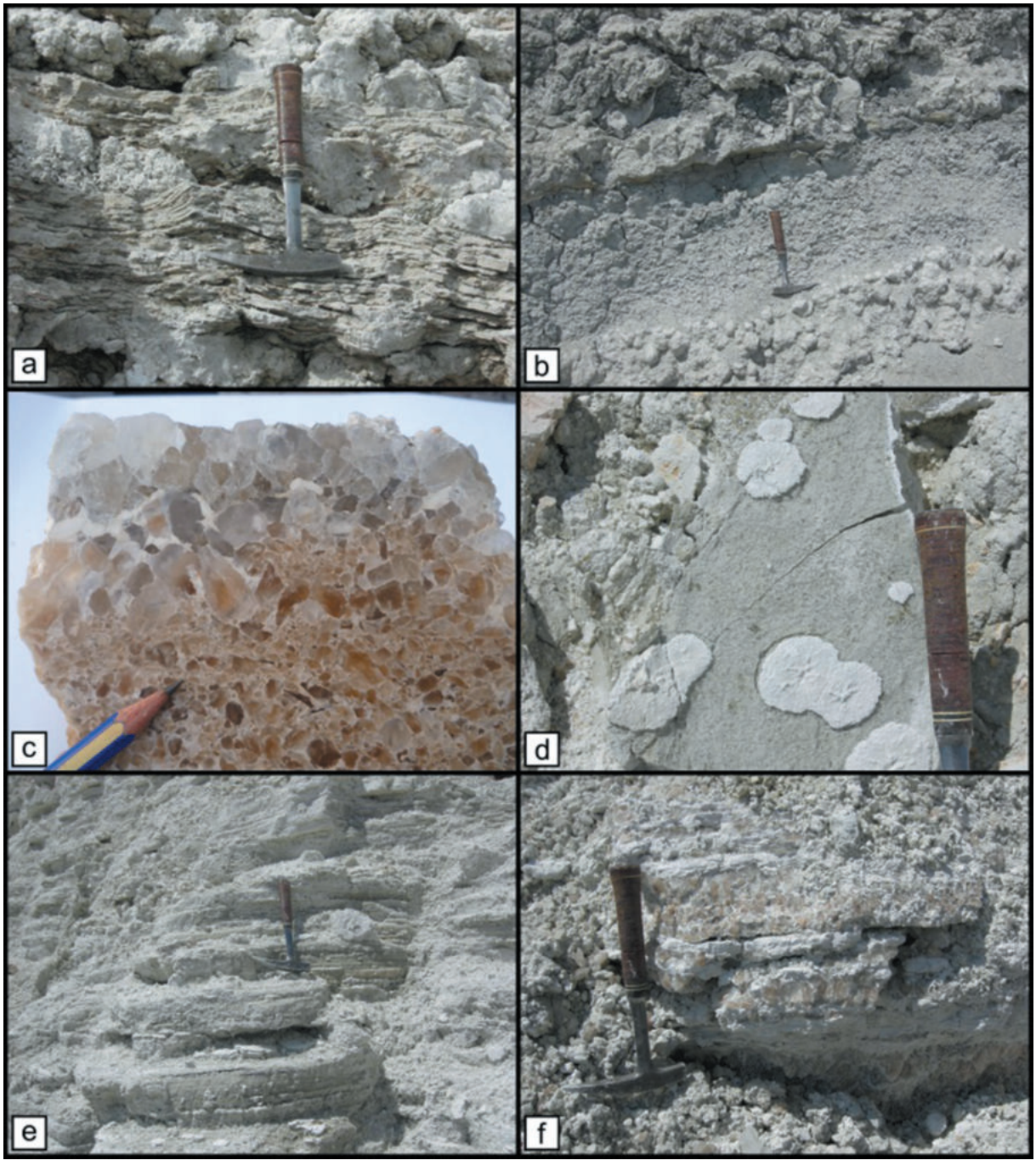

Figure 9. (a, b) Ulexite layers alternating with nodular and massive lithofacies of colemanite in the upper section of the Kırka Sarıkaya opencast deposit. Crystalline masses, vug porosity, geodic areas and cemented fractures can be observed; (c) Massive crystalline borax lithofacies. Borax crystals are transparent and rectangular to equant and are surrounded by a silt/clay matrix. The borax crystals at the top of the specimen are zoned. (d, e) Laminated lithofacies of borax (brown material) alternating with dolomitic, marly laminae (white laminae). (f) Laminated borax lithofacies with palisade fabric in borax laminae. Clear material corresponds to lutitic matrix and laminae (dolomitic claystone). Dark material corresponds to fresh, crystalline borax.

dolomitic/smectite claystones. The borax crystal beds typically display laminated and banded lithofacies consisting of alternating planar laminae of clay-rich sediment (<1 cm thick) and bands (1 cm to a few dm thick) of borax (Figure 9(a)). The borax forms <1 mm to 1 cm crystals that are euhedral to subhedral, transparent to brownish, and can show growth zoning formed by inclusions of the clay-rich matrix (Figure 9(b)). The borax crystal layers are separated 20–50-cm-thick layers of marl- and clay-rich matrix that contain coarse borax crystals (up to several cm). These crystals are euhedral and transparent, and generally devoid of internal zoning.

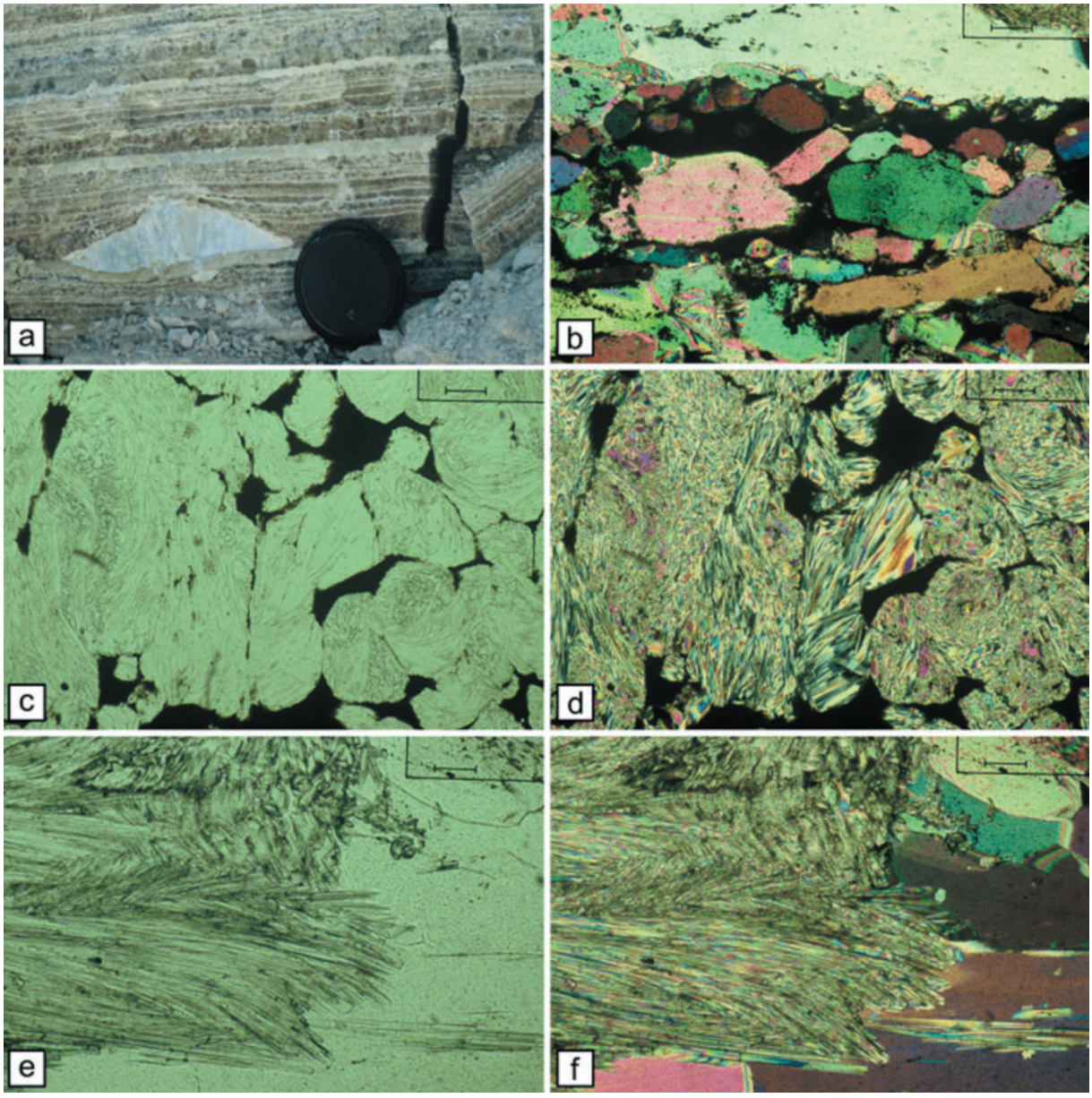

Figure 10. (a) Laminated lithofacies of borax (brown material) alternating with dolomitic, marly laminae (white laminae). Palisade fabric (bottom-nucleated, upward-directed, competitively grown crystals) can be seen in some borax laminae. In the lower part, a discoidal nodule of fibrous ulexite is present. The growth of this nodule is early diagenetic, being coeval with the borax laminae. Lens cap: 6 cm. (b) Photomicrographs of borax laminae. In the central lower part, the borax crystals are oriented parallel to bedding and are embedded in matrix (dark material). In the upper part, a large borax crystal is present, which shows pressure-solution features in contact with the small borax crystals underneath. Scale bar: 0.32 mm, crossed nicols) (Sarıkaya deposit). (c, d) Photomicrographs of pseudomorphs of fibrous ulexite after (precursor) borax. Note the various orientations and fascicular arrangements, the variable size, and the deformation features of ulexite fibres within the pseudomorphs. The photomicrograph corresponds to a zone close to the contact between the ulexite nodule and the borax laminae in A. Scale bar: 0.32 mm. (C: normal light; D: crossed nicols). (e, f) Photomicrographs of ulexite fibres replacing borax crystals, in the contact zone between a ulexite nodule and a borax lamina. Scale bar: 0.32 mm. (E: normal light; F: crossed nicols) (Sarıkaya deposit).

There is also a massive crystalline lithofacies of matrix-free, subhedral to anhedral, transparent crystals of borax, which form layers up to several metres thick. The borax crystals range between 1 and 2 cm in size with no particular orientation.

Within the borax laminae, two crystal fabrics may be distinguished. The palisade fabric is formed by matrix-poor, brown-coloured crystals up to 1–2 cm high, which are arranged in a subvertical fabric (Figure 10(a)). These crystals exhibit a planar base and an euhedral apex; dissolution

surfaces can be observed locally at the top of the crystals. In the unorientated fabric, the crystals are euhedral to anhedral and are surrounded by sediment matrix resulting in a clastic appearance. Locally, there is a tendency to normal grading and in some laminae; prismatic to tabular crystals are arranged parallel to the lamination, suggesting a cumulate origin. The laminated borax lithofacies frequently show an upward transition from palisade to unorientated fabrics, and both fabrics types are replaced locally by ulexite pseudomorphs after borax (Figures 9(a,e,f) and Figure 10(d)). The borax laminae also contain some ulexite nodules, which have planar bases and convex top surfaces, with the borax laminae thinning and deforming around the top surfaces of the nodules, suggesting that the ulexite nodules were coeval with accumulation of the borax laminae. The laminated lithofacies indicate subaqueous precipitation and the palisade fabric suggests a competitive bottom growth, whereas the matrix-rich crystals with unorientated fabric suggest more variable precipitation conditions (Figure 10(a)). The normal grading likely reflects subtle changes in the chemistry of lake brine (e.g. Helvacı and Ortí 2004).

The massive, crystalline borax lithofacies are most compatible with precipitation in a matrix-free and limited sediment input to the deeper basin. On the other hand, the clay inclusions in the interstitially grown, macrocrystalline lithofacies indicate they formed below the sediment-water interface. The borate lithofacies as a whole are enclosed by calcite and limestone facies that formed a resistant cap-rock to the borate zone.

Accessory minerals include celestite, gypsum, realgar and orpiment that occur in some borate layers. In addition, boron-bearing authigenic K-feldspar, smectite and illite occur in the tuffaceous horizons, accompanied by volcanic-derived sanidine, albite, anorthoclase, quartz, and secondary calcite (Helvacı *et al*. 1993). In the main ore, authigenic K-feldspar likely formed at the expense of primary clay or volcanic glass. The clays in the borate formation are also Mg-rich (up to 11 wt.% MgO) and are surrounded by thick carbonate mounds and extensive calcite.

The clay layers are composed of smectite-group minerals (mainly hectorite) and, less frequently, illite and chlorite minerals; these layers also contain some volcanic tuffs (commonly altered to zeolites), quartz, biotite, and feldspar (Helvacı *et al*. 1993). Dolomite is the main carbonate mineral accompanying the clay; minor amounts of magnesite, strontianite and calcite are also present (Helvacı *et al*. 1993; Çolak 1995).

Overall, the various borax lithofacies reflect evolution from a predominantly subaqueous setting with variable water depths (perennial lake stage) in the lower part, to an ephemeral setting (playa-lake stage), before reverting to a subaqueous setting in the upper part. Evaporative concentration of the boron-rich solutions in the paleo lake, together with periodic changes in temperature of the water mass, is considered to be the main controls on the borax crystallization (Bowser 1965).

Therefore, the borate mineral zoning observed in the deposit is considered to be a primary depositional feature; not only for borax and ulexite, but also for the colemanite and the Mg borates overlying the central body. This zoning thus represents the evolution of a Na-rich boratiferous saline lake, with a lateral gradient of salinity due to mixing with dilute groundwater responsible for the concentric pattern (Figure 11, Helvacı and Ortí 2004; Helvacı and Palmer 2017).

Stratigraphic, geomorphic and structural studies in the borate area and throughout the Kırka Basin, suggest that the borate formation underwent only moderate burial after its accumulation (<300 m), as is typical of other borate-bearing Neogene basins in western Turkey (Helvacı and Alonso 2000). However, the Kırka-Sarıkaya deposit differs from similar borax deposits at Boron, California, and Tincalayu, Argentina, in having very little inter-crystalline clay (Bowser 1965; Alonso 1986; Alonso *et al*. 1988; Kistler and Helvacı 1994).

2.7. Kırka Göcenoluk borate deposit

Exploratory drilling in 2008–2009 in the Göcenoluk area 10 km northwest of the Kırka Sarıkaya open-pit mine intersected a 500-m-thick succession of limestones, dolostones, tuffs and three borate-bearing units (Figures 7 and 8). Ignimbrites and volcaniclastic deposits are the dominant lithologies in the bottom 700 m of the northernmost borehole (BMK-2008-7). These rocks are overlain by a sequence of clays, marls and limestones deposited in the Middle Miocene (Floyd *et al*. 1998; Helvacı and Ortí 2004; Garcia-Veigas and Helvacı 2013) in the northern sequence between BMK-2008-2 and BMK-2009-3 (Figure 8). Southward, the lithologies of boreholes BMK-2008-4 and 6 predominantly consist of a sequence of clay, marls and limestone, suggesting an association of distal fluvial and carbonate deposition (e.g., McLane 1995). There are also volcaniclastic deposits at the bottom of the drill core. The southernmost borehole (BMK-2008-7) shows a similar lithology with the northern boreholes with an upper sequence of epiclastic deposits (García-Veigas and Helvacı 2013; Seghedi and Helvacı 2014) (Figure 8).

The borate succession in the 2008–6 borehole is mainly formed by an upper probertite unit (~100 m thick) which overlies a lower borax unit (~100 m thick). Abundant small tunellite crystals are scattered throughout the sequence. The basal borax unit consists of massive beds of anhedral cm-sized crystals interbedded with tuffs and dolomites. In both units, the borates show

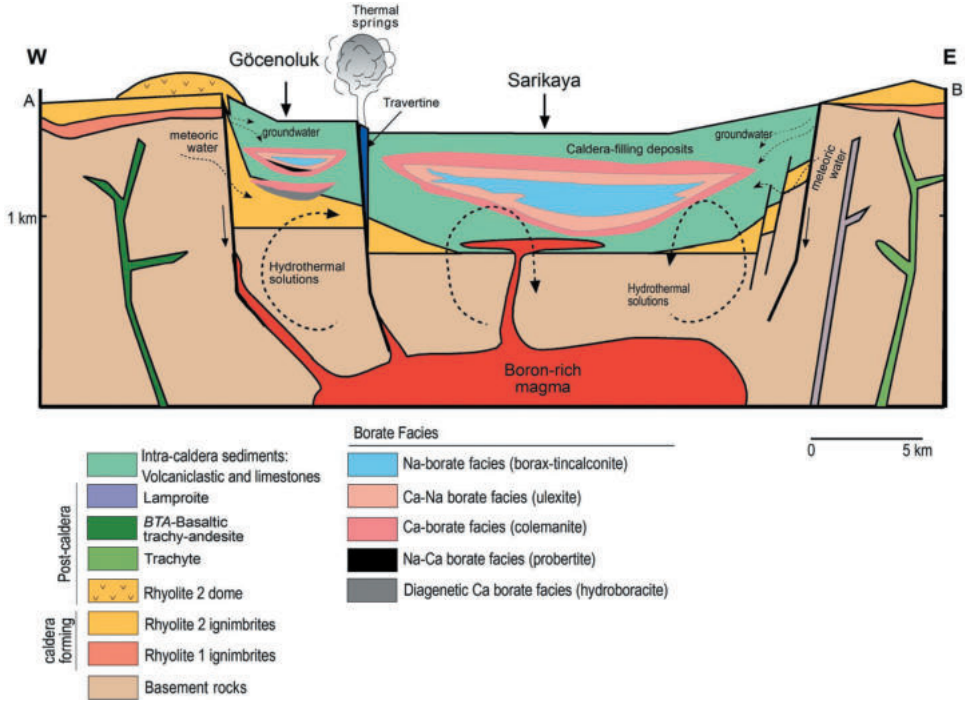

Figure 11. Model of the borate deposition (ca. 16–18 Ma) in the Early Miocene Kırka-Phrigian Caldera basin (see Figure 3 for section line A-B and explanations in the text).

evidence of interstitial growth breaking and deforming peloidal dolomite and stromatolitic layers.

The three borate units are composed of Ca-Na-borates (probertite and ulexite) and are designated as: (1) the Lower Borate Unit (LBU), up to 70 m thick consisting of probertite with a basal hydroboracite bed, (2) the Intermediate Borate Unit (IBU), up to 150 m thick consisting of ulexite in borehole 2009–1 and probertite in borehole 2008–6; and (3) the Upper Borate Unit (UPU), up to 120 m thick, consisting of probertite–ulexite overlain by a colemanite bed in borehole 2008–6 and by a colemanite–hydroboracite bed in borehole 2009–1 (Figures 7 and 8; Garcia-Vegias and Helvacı 2013). The Na-borate (borax) intervals in the Intermediate Borate Unit are used for lithostratigraphic correlation of the boreholes.

Ca-Na-borates ulexite (Figure 7) and probertite (Figure 8) are the most abundant borates. Both minerals occur as white to brownish, sub-mm size fibres that exhibit a silky lustre (Figure 8). The borate textures include micronodular, nodular, vertically elongated (columnar), and massive, all of which may grade into one another. Finely laminated carbonate, mainly dolostone, is the most abundant lithology in the Göcenoluk succession and consists of white, pure, cm-thick laminae of fine-grained, unorientated, platy euhedral crystals of dolomite. Ulexite micronodules occur within dolomite laminae of the stromatolites (García-Veigas and Helvacı 2013). Dolomite layers commonly exhibit grading from pure crystalline dolostone to a borate-rich matrix containing dispersed dolomite crystals and microbial-mediated dolomite aggregates (García-Veigas and Helvacı 2013).

Colemanite is the only borate mineral observed in outcrops in the Göcenoluk area (İnan *et al*. 1973), where it occurs as discrete intervals at the top and/or base of the three borate units in the studied boreholes (Figures 7 and 8; García-Veigas and Helvacı 2013). Colemanite exhibits massive-nodular (Figure 9) and poorly banded lithofacies. These lithofacies contain colemanite nodules made up of prismatic-radiating crystals with a marked strontium zonation (Figures 9 and 10). Some dolomite crystals are scattered within colemanite beds. The colemanite nodules do not show evidence of having grown among broken dolomite layers, in contrast to the ulexite–probertite occurrences (García-Veigas and Helvacı 2013).

Na-borates are represented by borax and tincalconite, and kernite is rare or absent in this area. Borax is commonly altered to tincalconite in the Göcenoluk borehole cores and exhibits poorly defined banding irregularly interlayered with tuffs and carbonates. Borax intervals, up to 10 m in thickness, exhibit a chaotic fabric in which the borax crystals are

surrounded by dolomite, and also include films of contorted dolomite. Isolated borax crystals and crystal clusters grew displacively and deformed the associated laminated carbonates suggesting interstitial growth. No cumulate crystalline fabrics, such as those recognized in the Sarıkaya succession (Helvacı and Ortí 2004), were observed in the Göcenoluk boreholes. Radial aggregates of probertite replacing borax also occur in the borax beds (Figure 9) (García-Veigas and Helvacı 2013).

Minor borate minerals include hydroboracite (Ca-Mg-borate) and tunellite (Sr-borate). Hydroboracite ($CaMg(B_6O_8(OH)_6).3H_2O$) is most common in the colemanite beds, where it occurs as discrete porphyroblasts and fibrous aggregates replacing colemanite. The massive hydroboracite at the base of the LBU is composed of coalesced nodules containing colemanite relicts. Tunellite ($Sr(B_6O_9(OH)_2).3H_2O$) and rare veatchite-A ($Sr_2(B_{11}O_{16}(OH)_5).H_2O$) (Kumbasar 1979) occur as; (1) bladed crystals cementing macrophyte components in carbonate travertine, (2) septarian fills of colemanite vugs, and (3) as microcrystalline replacement of colemanite, ulexite and borax. Hydroboracite, tunellite and veatchite-A are all interpreted as early diagenetic replacements of primary borates in the presence of Mg^{2+}- and Sr^{2+}-rich brines (García-Veigas and Helvacı 2013). Searlesite ($NaBSi_2O_5(OH)_2$) is the most important authigenic mineral and is found in both the volcaniclastic and authigenic clay layers (García-Veigas and Helvacı 2013).

Volcaniclastic layers within the borate-bearing units mainly consist of fine-grained tuffs (0.2–5 mm). Pumice and glass-shards are rare because they are generally altered to clay, zeolite (mainly analcime) and searlesite. Pyroclastic layers consist of coarse-grained tuffs (-<64 mm) with vitroclastic–porphyritic textures. They contain pumice fragments, volcanic glass shards and basement fragments. The tuff layers between the borate-bearing units have been moderately zeolitized to heulandite (Ca-Na-zeolite) and minor clinoptilolite (Na-K-Ca-zeolite). The neoformed clay fraction is comprised of Mg-rich smectite, and minor illite and chlorite.

Petrographic observations of both probertite and colemanite indicates that they are primary precipitates which grew interstitially in volcaniclastic sediments and soft dolomitic muds deposited on the bottom of the paleolake. Intense water-rock interaction with volcano-sedimentary layers induced the dissolution of K-feldspar and plagioclase, and their replacement by probertite. Abundant analcime and searlesite formed as a consequence of the leaching of silica from the silicates. The absence of laminated borax in this marginal position suggests that it also formed below the paleolake water-sediment interface.

3. Discussion

3.1. Volcanic evolution and Kırka-Phrigian caldera collapse

Caldera collapse results from large explosive volcanic eruptions, and though there are a variety of caldera morphologies, they invariably form initially by down-sagging followed by a piston-like subsidence bounded by nearly vertical ring faults (e.g. Komuro *et al*. 1984; Komuro 1987; Martí *et al*. 1994; Roche *et al*. 2000; Cole *et al*. 2005).

Seghedi and Helvacı (2016) suggest that changes in lithology in closely spaced boreholes indicate that the floor of the Kırka-Phrigian caldera was uneven and is now located ~1000–1200 m below the present surface. However, because complete exploration of the caldera interior requires more drilling, the details of caldera subsidence physiognomy are still uncertain. Nevertheless, the subsided collapse block controlled the locus of lake sedimentation that resulted in infilling of both the Sarıkaya and Göcenoluk sub-basins. Transport directions of volcaniclastic deposits are oriented towards the interior of the caldera, and define the caldera margins as the main source of this material. The limestone deposition may represent periods of tectonic calm with reduced physical erosion that facilitated carbonate precipitation in the isolated caldera basin.

3.2. Borate mineralization within Caldera Basin

Post-caldera hydrothermal systems are common in calderas worldwide (e.g., Cole *et al*. 2005; Ulusoy *et al*. 2008; John 2008; Kennedy *et al*. 2012; Henry and John 2013), so it is almost certain that the post-caldera activity identified here drove vigorous hydrothermal systems. The heat, volatiles and structural pathways provided by the hydrothermal fluids generated an initially large area of silica deposition and veining along ring fault structures, followed by borate mineralization and deposition, and in the final stage deposition of large travertine deposits along N-S fault structures that clearly post-date the caldera formation. The fluids within the post-caldera hydrothermal system were likely enriched in the magmatic volatiles that transported boron to the borate deposits. The volcanism also likely supplied B (and other mobile elements such as As, F, Li, Sb) to the caldera-basin sediments by leaching of volcanic rocks by hot meteoric waters and as well as post-caldera hydrothermal degassing (e.g. Kistler and Helvacı 1994; Floyd *et al*. 1998; Helvacı and Alonso 2000; García-Veigas and Helvacı 2013; Seghedi and Helvacı 2016; Helvacı and Palmer 2017; Benson *et al*. 2017). The two most likely sources/origins for B and other elements enriched in these deposits are: (1) degassing of residual or resurgent

magmas (perhaps represented by the rhyolite 2 ring fracture domes or by unexposed intrusions at depth beneath the caldera), and/or (2) leaching of the ignimbrites filling the caldera and/or secondary volcaniclastic deposits.

The borate mineralization formed by evaporation of boron-enriched lake water after accumulating in the caldera lake basin (Helvacı 1995; Seghedi and Helvacı 2016). The boron isotope data are consistent with colemanite precipitated from a brine of lower pH (average 8.2) under more acidic conditions than ulexite (8.6), with borax precipitated from a brine of higher pH (8.83) than ulexite (Palmer and Helvacı 1995); i.e. the different borate minerals did not form at the same time and place. The Kırka borate deposition succession is as follows: colemanite – ulexite – borax – ulexite – colemanite, with the thickness of colemanite and ulexite zones being much thinner than the borax zone (Figure 7). The borate basin in the Kırka area was dominantly surrounded by rhyolitic ignimbrites, so the borate lake would have been predominantly fed by Na-rich rather than Ca-rich fluids, which explains why the borax zone is much thicker than the ulexite and colemanite zones (Figure 8). There are also carbonate layers in the basin as mentioned formed from Ca-rich fluid below and upper part of the borate zone. Travertine was a later phase in the deposit cross-cutting all the sections including upper limestones in the deposit (see Figure 6(e,f)).

The Kırka borate deposits represent the end-product of four stages of transportation and deposition of B: (a) initial concentration in magmatic fluids; (b) incorporation in continental crust via subalkaline-potassic-ultrapotassic magmatism (e.g. Yücel-Öztürk *et al*. 2012; Palmer *et al*. 2019), (c) melting of B-enriched continental crust to produce ignimbrites; and (d) selective mobilization of B from ignimbrites by local hydrothermal activity and precipitation in alkaline caldera lakes. Finally, although the initial enrichment of B in volcanic source rocks is a necessary feature for the development of borates, the local climatic, tectonic and volcanic conditions are also critical features in their eventual genesis (Floyd *et al*. 1998; Helvacı and Palmer 2017).

In general, the borate minerals form as primary precipitates from Ca-rich to Na-rich waters towards the centre of the closed caldera lakes (Figure 11). In the Göcenoluk succession, a similar but rapid lateral change in fluid composition and frequent influx of clastic material intercalated with borate minerals were present together with increasing alkalinity. The model illustrated in Figure 10 includes a marginal lacustrine carbonate, with the borate minerals mainly forming during lake shrinkage and during water table drawdown in the closed caldera basin. The major differences between Sarıkaya and Göcenoluk areas are that subaqueous precipitation of borax occurred in Sarıkaya, whereas there are abundant carbonate sediments as well as multiple cycles of boron mineral deposition in the Göcenoluk area. These differences (as well as other sedimentological features) suggest that the two deposits formed in separate sub-basins within the caldera, with only limited burial diagenesis since their formation.

4. Conclusions

Formation of the world-class Kırka borate deposit in the northernmost part of the Miocene Eskişehir–Afyon volcanic field, Anatolia, is intimately related to development of a large caldera formed by eruption of a rhyolite ignimbrites at ~18.9 Ma. The eruption and subsequent caldera collapse formed a roughly elliptical (24 km x 15 km) depression ~1000 m deep ringed by outflow ignimbrites. A second eruptive period at 18.7–18.63 Ma was dominantly effusive forming rhyolite domes and lava flows and was closely associated with filling of the caldera by volcaniclastic deposits and precipitation of limestones. The last volcanic event at 16.92–16.21 Ma consisted of minor volumes of basaltic trachy andesite and lamproite lavas.

Post-volcanic activity – following ~N-S faulting – was dominated by hydrothermal activity with world-class borate formation during basin generation and late-stage travertine deposition. Leaching of the local ignimbrites by hot meteoric waters and post-caldera hydrothermal degassing were likely the primary sources of the boron. Based on differences in their borate mineralogy and sedimentological evolution, it is likely that the Kırka Sarıkaya and Göcenoluk borate deposits formed in separate sub-basins within the large caldera.

Acknowledgments

This work was supported by the Dokuz Eylül University Scientific Project (Bilimsel Araştırma Projesi) No: 2010.KB. FEN.009. We recognize the assistance of Yasin Aydın during the field study and Halil Danabaş and Ferhan Eren during logging. We thank Mustafa Helvacı and Berk Çakmakoğlu for their typing and drafting assistance. We are grateful to Bill Griffin for his helpful suggestions. We also thank the Eti Mine Company General Management for their logistic support during the field study and for their permission to publish the simplified lithology of the borehole data. I.S. was supported by grant of Ministry of Research and Innovation, CNCS – UEFISCDI, project number PN-III-P4-ID-PCCF-2016-4-0014, within PNCDI III. We gratefully appreciate three reviewers for their help in clarifying the ideas presented in this manuscript. Thorough editorial handling by Dr. Robert J. Stern (Editor-in-

Chief) is appreciated.

Disclosure statement

No potential conflict of interest was reported by the authors.

Funding

This work was supported by the Dokuz Eylül University Scientific Project [2010.KB. FEN.009]; grant of Ministry of Research and Innovation, CNCS – UEFISCDI [PN-III-P4-ID-PCCF -2016-4-0014, within PNCDI III].

References

Akal, C., Helvacı, C., Prelević, D., and van den Bogaard, P., 2013, High-K volcanism in the Afyon region, western Turkey: From Si-oversaturated to Si-undersaturated volcanism: International Journal of Earth Sciences, v. 102, no. 2, p. 435–453. doi: 10.1007/s00531-012-0809-9

Alonso, R.N., 1986, Ocurrencia, posición estratigráfcia y génesis de los depósitos de boratos de la región de la Puna Argentina: [Ph. D. Thesis]: Salta, Argentina, Universidad Nacional de Salta, 196 p.

Alonso, R.N., Helvacı, C., Sureda, R.J., and Viramonte, J.G., 1988, A new Tertiary borax deposit in the Andes: Mineralium Deposita, v. 23, no. 4, p. 299–305. doi: 10.1007/BF00206411

Anderson, D., 1997, The relationship between magmatism and borate mineralisation in Western Turkey: [PhD Thesis]: Leicester, United Kingdom, The University of Leicester, 138 p.

Aydar, E., Bayhan, H., and Gourgaud, A., 1998, Köroğlu caldera, mid-west Anatolia, Turkey: Volcanological and magmatological evolution: Journal of Volcanology and Geothermal Research, v. 85, no. 1–4, p. 83–98. doi: 10.1016/S0377-0273(98)00051-1

Benson, T.R., Coble, M.A., Rytuba, J.J., and Mahood, G.A., 2017, Lithium enrichment in intracontinental rhyolite magmas leads to Li deposits in caldera basins: Nature Communications, v. 8, no. 1, p. 1–9. doi:10.1038/s41467-017-00234-y

Bowser, C.J., 1965, Geochemistry and petrology of the sodium-borates in the non-marine evaporite environment. [Ph.D. Thesis]: Los Angeles, USA, The University of California, 282 p.

Çemen, İ., Helvacı, C., and Ersoy, E.Y., 2014, Cenozoic extensional tectonics in western and central Anatolia, Turkey: Introduction: Tectonophysics, v. 635, p. 1–5.

Çolak, M., 1995, The Emet and Kırka borate mines (Turkey). 1: Mineralogy and chemistry of the clays. 2: Ceramic application of their tailing products: Fribourg, Switzerland, The University of Fribourg. 214 p.

Cole, J.W., Milner, D.M., and Spinks, K.D., 2005, Calderas and caldera structures: A review: Earth-Science Reviews, v. 69, p. 1–26.

Dilek, Y., and Altunkaynak, Ş., 2009, Geochemical and temporal evolution of Cenozoic magmatism in western Turkey: Mantle response to collision, slab break-off, and lithospheric tearing in an orogenic belt, in van Hinsbergen, D.J.J., Edwards, M.A., and Govers, R. eds., Collision and collapse at the Africa–Arabia–Eurasia subduction zone. Geological Society, Vol. 311: London, Special Publications, p. 213–233.

Dilek, Y., and Altunkaynak, Ş., 2010, Geochemistry of neogene-quaternary alkaline volcanism on western Anatolia, Turkey, and implications for the Aegean mantle: International Geology Review, v. 52, p. 631–655.

Erkül, F., and Erkül, S.T., 2010, Geology of the Early Miocene Alaçamdağ magmatic complex and implications for the western Anatolian extensional tectonics: Bulletin of the Mineral Research and Exploration Institute of Turkey, v. 141, p. 1–25.

Ersoy, E.Y., Helvacı, C., and Palmer, M.R., 2010, Mantle source characteristics and melting models for the early-middle Miocene mafic volcanism in Western Anatolia: Implications for enrichment processes of mantle lithosphere and origin of K-rich volcanism in post-collisional settings: Journal of Volcanology and Geothermal Research, v. 198, p. 112–128.

Ersoy, E.Y., and Palmer, M.R., 2013, Eocene–Quaternary magmatic activity in the Aegean: Implications for mantle metasomatism and magma genesis in an evolving orogeny: Lithos, v. 180–181, p. 5–24.

Floyd, P.A., Helvacı, C., and Mittevede, S.K., 1998, Geochemical discrimination of volcanic rocks associated with borate deposits: An exploration tool?: Journal of Geochemical Exploration, v. 60, p. 185–205.

García-Veigas, J., and Helvacı, C., 2013, Mineralogy and sedimentology of the Miocene Göcenoluk borate deposit, Kırka district, western Anatolia, Turkey: Sedimentary Geology, v. 290, p. 85–96.

Garrett, D.E., 1998, Borates, handbook of deposits, processing, properties and use: California, Academic Press, 483 p.

Helvacı, C., 1995, Stratigraphy, mineralogy, and genesis of the Bigadiç borate deposits, western Turkey: Economic Geology, v. 90, p. 1237–1260.

Helvacı, C., and Alonso, R.N., 2000, Borate deposits of Turkey and Argentina: A summary and geological comparison: Turkish Journal of Earth Sciences, v. 9, p. 1–27.

Helvacı, C., and Ortí, F., 2004, Zoning in the Kırka borate deposit, western Turkey: Primary evaporitic fractionation or diagenetic modifications?: The Canadian Mineralogist, v. 42, p. 1179–1204.

Helvacı, C., and Palmer, M.R., 2017, Origin and distribution of evaporitic borates: The primary economic sources of boron: Elements, v. 13, no. 4, p. 249–254.

Helvacı, C., Stametakis, M.G., Zagouroglou, C., and Kanaris, J., 1993, Borate minerals and related authigenic silicates in northeastern Mediterranean Late Miocene continental basins: Exploration Mining Geology, v. 2, p. 171–178.

Helvacı, C., Yücel-Öztürk, Y., and Emmermann, A., 2017, Fluorescence survey of Turkish borate minerals: Comparative measurements of fluorescence spectra of the most important borate mıneral species, Turkey: Journal of Mineralogy and Geochemistry, v. 194, no. 1, p. 1–17.

Henry, C.D., and John, D.A., 2013, Magmatism, ash-fl ow tuffs, and calderas of the ignimbrite flareup in the western Nevada volcanic fi eld, Great Basin, USA: Geosphere, v. 9, no. 3, p. 951–1008.

İnan, K., 1972, New borate district, Eskişehir–Kırka Province, Turkey: Transactions of the Institution of Mining and Metallurgy (Section B Appled Earth Science), v. 81, p. 163–165.

İnan, K., Dunham, A.C., and Esson, J., 1973, Mineralogy, chemistry and origin of Kırka borate deposit, Eskishehir Province, Turkey: Transactions of the Institution of Mining and Metallurgy (Section B Appled Earth Science), v. 82, p. 114–123.

John, D.A., 2008, Supervolcanoes and Metallic Ore Deposits: Elements, v. 4, p. 22.

Karacık, Z., Yılmaz, Y., and Pearce, J.A., 2007, The Dikili-Çandarlı volcanics, Western Turkey: Magmatic interactions as recorded by petrographic and geochemical features: Turkish Journal of Earth Sciences, v. 16, p. 493–522.

Karaoğlu, Ö., Helvacı, C., and Ersoy, E.Y., 2010, Petrogenesis and $^{40}Ar/^{39}Ar$ geochronology of the volcanic rocks of the Uşak-Güre basin, western Türkiye: Lithos, v. 119, p. 193–210.

Keller, J., and Villari, L., 1972, Rhyolitic ignimbrites in the region of Afyon (Central Anatolia): Bulletin Volcanologique, v. 36, p. 342–358.

Kennedy, B., Wilcock, J., and Stix, J., 2012, Caldera resurgence during magma replenishment and rejuvenation at Valles and Lake City calderas: Bulletin of Volcanology, v. 74, p. 1833–1847.

Kistler, R.B., and Helvacı, C., 1994, Boron and borates, *in* Carr, D. D. ed., Industrial minerals and rocks, 6th ed.: Society for Mining, Metallurgy & Exploration Inc.: Switzerland, Springer, p. 171–186.

Koç, Ş., Kavrazlı, Ö., and Koçak, İ., 2017, Geochemistry of Kestelek Colemanite Deposit, Bursa, Turkey: Journal of Earth Science, v. 28, no. 1, p. 63–77.

Koçak, İ., and Koç, Ş. 2012, Kırka Borat Yatağında Zenginleşen Eser Elementler. V. Ulusal Jeokimya Sempozyumu, in Bildiriler ve Özetler Kitabı, 23-25 May, Denizli, Türkiye, p. 43–44.

Koçak, İ., and Koç, Ş., 2016, Geochemical characteristics of Kırka (Sarıkaya) borate deposit, northwestern Anatolia, Turkey: J. Earth Syst. Sci., v. 125, no. 1, p. 147–164.

Koçak, İ., and Koç, Ş., 2018, Geochemical characteristics of The Emet (Espey-Hisarcik) borate deposits, Kütahya, Turkey: Journal of African Earth Sciences, v. 142, p. 52–63.

Komuro, H., 1987, Experiments on cauldron formation: A polygonal cauldron and ring fractures: Journal of Volcanology and Geothermal Research, v. 31, no. 1–2, p. 139–149.

Komuro, H., Fujita, Y., and Kodama, K., 1984, Numerical and experimental models on the formation mechanism of collapse basins during the Green Tuff orogenesis of Japan: Bulletin of Volcanology, v. 47, no. 3, p. 649–666.

Kumbasar, I., 1979, Veatchite-A, a new modification of veatchite: American Mineralogis, v. 64, p. 362–366.

Lavallée, Y., Dingwell, D.B., Johnson, J.B., Cimarelli, C., Hornby, A.J., Kendrick, J.E., von Aulock, F.W., Kennedy, B.M., Andrews, B.J., Wadsworth, F.B., Rhodes, E., and Chigna, G., 2015, Thermal vesiculation during volcanic eruptions: Nature, v. 528, p. 544–547.

Martí, J., Mitjavila, J., and Araña, V., 1994, Stratigraphy, structure and geochronology of the Las Cañadas caldera (Tenerife, Canary Islands): Geological Magazine, v. 131, no. 6, p. 715–727.

McLane, M., 1995, Sedimentology: New York, Oxford University Press, 423 p.

Okay, A.İ., 2011, Tavşanlı zone: The northern subducted margin of the Anatolide- Tauride block: Bulletin of the Mineral Research and Exploration, v. 142, p. 191–221.

Okay, A.İ., and Satır, M., 2006, Geochronology of Eocene plutonism and metamorphism in northeast Turkey: Evidence for a possible magmatic arc: Geodinamica Acta, v. 19, no. 5, p. 251–266.

Özcan, A., Göncüoğlu, M.C., Turan, N., Uysal, Ş., Şentürk, K., and Işık, A., 1988, Late Paleozoic evolution of the Kütahya-Bolkardağ belt: Middle East Technical University: Journal of Pure and Applied Sciences, v. 21, p. 211–220.

Özkul, C., 2008, Emet (Kütahya) Neojen Havzası Bor Prospeksiyonu: Hedef Saptamada Jeokimyasal Yöntem Geliştirme, Kocaeli Üniversitesi, Fen Bilimleri Enstitüsü. Kocaeli, Doktora Tezi, 158 pp. (unpublished)

Özkul, C., Çiftçi, E., Tokel, S., and Savaş, M., 2017, Boron as an exploration tool for terrestrial borate deposits: A soil geochemical study in neogene emet-hisarcik basin where the world largest borate deposits occur (Kütahya-Western Turkey): Journal of Geochemical Exploration, v. 173, p. 31–51.

Palmer, M.R., Ersoy, E.Y., Akal, C., Uysal, I., Genç, S.C., Banks, L.A., Cooper, M.J., Milton, J.A., and Zhao, K.D., 2019, A short, sharp pulse of potassium-rich volcanism during continental collision and subduction: Geology, v. 47, p. 1079–1082.

Palmer, M.R., and Helvacı, C., 1995, The boron isotope geochemistry of the Kırka borate deposit, western Turkey: Geochimica et cosmochimica acta, v. 59, no. 17, p. 3599–3605.

Prelević, D., Akal, C., Foley, S.F., Romer, R.L., Stracke, A., and Van Den Bogaard, P., 2012, Ultrapotassic mafic rocks as geochemical proxies for post-collisional Dynamics of orogenic lithospheric mantle: The case of southwestern Anatolia, Turkey: Journal of Petrology, v. 53, p. 1019–1055.

Purvis, M., and Robertson, A.H.F., 2005, Miocene sedimentary evolution of the NE-SW-trending Selendi and Gördes Basins, Western Turkey: Implications for extensional processes: Sedimentary Geology, v. 174, p. 31–62.

Roche, O., Druitt, T.H., and Merle, O., 2000, Experimental study of caldera formation: Journal of Geophysical Research, v. 105, no. B1, p. 395–416.

Savaşçın, Y., and Oyman, T., 1998, Tectono–magmatic evolution of alkaline volcanics at the Kırka–Afyon–Isparta structural trend, Sw Turkey: Turkish Journal of Earth Sciences, v. 7, p. 201–214.

Seghedi, I., Ersoy, E.Y., and Helvacı, C., 2013, Miocene–Quaternary volcanism and geodynamic evolution in the Pannonian Basin and the Menderes Massif: A comparative study: Lithos, v. 180-181, p. 25–42.

Seghedi, I., and Helvacı, C., 2016, Early Miocene Kırka-Phrigian Caldera, western Turkey (Eskişehir province), preliminary volcanology, age and geochemistry data: Journal of Volcanology and Geothermal Research, v. 327, p. 503–519.

Şengör, A.M.C., and Yılmaz, Y., 1981, Tethyan evolution of Turkey: A plate tectonic approach: Tectonophysics, v. 75, p. 181–241.

Smith, G.I., and Medrano, M.D., 1996, Continental borate deposits of Cenozoic age, *in* Grew, E.S., and Anovitz, L.M. eds., Boron: Mineralogy, petrology and geochemistry, Reviews in Mineralogy, Mineralogical Society of America, v. 33, p. 263–298.

Sunder, M.S., 1980, Geochemistry of the Sarıkaya borate deposit (Kırka-Eskişehir): Bulletin of geological congress: Turkey, v. 2, p. 19–34.

Ulusoy, İ., Labuzuy, P., Aydar, E., Ersoy, O., and Çubukçu, E., 2008, Structure of the Nemrut caldera (Eastern Anatolia, Turkey) and associated hydrothermal fluid circulation: Journal of Volcanology and Geothermal Research, v. 174, p. 269–283.

Yalçın, H., 1988, Mineralogical-petrographic and geochemical investigation of volcano-sedimentary formations of Kırka (Eskişehir) region: PhD Thesis, Hacettepe University,

Institute of Graduate Studies in Science, Beytepe, Ankara, 209 p.

Yalçın, H., and Baysal, O., 1991, Kırka (Seyitgazi-Eskişehir) borat yataklarinin jeolojik konumu, dağılımı ve oluşumu: MTA Dergisi, v. 113, p. 93–104. (In Turkish)

Yılmaz, Y., Genç, Ş.C., Gürer, Ö.F., Bozcu, M., Yılmaz, K., Karacık, Z., Altunkaynak, Ş., and Elmas, A., 2000, When did the western Anatolian grabens begin to develop?, *in* Bozkurt, E., Winchester, J.A., and Piper, J.D.A. eds., Tectonics and magmatism in Turkey and the surrounding area: Geological Society of London, Vol. 173, p. 353–384.

Yücel-Öztürk, Y., Helvacı, C., and Satır, M., 2012, Geochemical and isotopic constraints on petrogenesis of the Beypazari granitoid, NW Ankara, Western Central Anatolia, Turkey: Turkish Journal of Earth Sciences, v. 21, p. 53–77.